

Electronic excitation in bulk and nanocrystalline alkali halides

Elena Bichoutskaia and Nicholas C. Pyper

Citation: *J. Chem. Phys.* **137**, 184104 (2012); doi: 10.1063/1.4764307

View online: <http://dx.doi.org/10.1063/1.4764307>

View Table of Contents: <http://jcp.aip.org/resource/1/JCPSA6/v137/i18>

Published by the [American Institute of Physics](#).

Additional information on *J. Chem. Phys.*

Journal Homepage: <http://jcp.aip.org/>

Journal Information: http://jcp.aip.org/about/about_the_journal

Top downloads: http://jcp.aip.org/features/most_downloaded

Information for Authors: <http://jcp.aip.org/authors>

ADVERTISEMENT



**ACCELERATE COMPUTATIONAL CHEMISTRY BY 5X.
TRY IT ON A FREE, REMOTELY-HOSTED CLUSTER.**

[LEARN MORE](#)

Electronic excitation in bulk and nanocrystalline alkali halides

Elena Bichoutskaia¹ and Nicholas C. Pyper²

¹*School of Chemistry, University of Nottingham, University Park, Nottingham NG7 2RD, United Kingdom*

²*University Chemical Laboratory, Lensfield Road, Cambridge CB2 1EW, United Kingdom*

(Received 3 August 2012; accepted 11 October 2012; published online 13 November 2012)

The lowest energy excitations in bulk alkali halides are investigated by considering five different excited state descriptions. It is concluded that excitation transfers one outermost halide electron in the fully ionic ground state to the lowest energy vacant s orbital of one closest cation neighbour to produce the excited state termed dipolar. The excitation energies of seven salts were computed using shell model description of the lattice polarization produced by the effective dipole moment of the excited state neutral halogen–neutral metal pair. *Ab initio* uncorrelated short-range inter-ionic interactions computed from anion wavefunctions adapted to the in-crystal environment were augmented by short-range electron correlation contributions derived from uniform electron-gas density functional theory. Dispersive attractions including wavefunction overlap damping were introduced using reliable semi-empirical dispersion coefficients. The good agreement between the predicted excitation energies and experiment provides strong evidence that the excited state is dipolar. In alkali halide nanocrystals in which each ionic plane contains only four ions, the Madelung energies are significantly reduced compared with the bulk. This predicts that the corresponding intra-crystal excitation energies in the nanocrystals, where there are two excited states depending on whether the halide electron is transferred to a cation in the same or in the neighbouring plane, will be reduced by almost 2 eV. For such an encapsulated KI crystal, it has been shown that the greater polarization in the excited state of the bulk crystal causes these reductions to be lowered to a 1.1 eV–1.5 eV range for the case of charge transfer to a neighbouring plane. For intra-plane charge transfer the magnitude of the polarization energy is further reduced thus causing the excitation in these encapsulated materials to be only 0.2 eV less than in the bulk crystal. © 2012 American Institute of Physics. [<http://dx.doi.org/10.1063/1.4764307>]

I. BACKGROUND

There is much interest, both experimental^{1–6} and theoretical,^{7–9} in the properties of nanocrystals prepared by encapsulation in single walled carbon nanotubes (SWNT). These constrain the structures of the encapsulated materials preventing them from reverting to the bulk structure. The structures of several of these encapsulated crystals have been accurately determined by recently developed methods in high resolution transmission electron microscopy.^{10,11} A few such crystals exhibit novel structures unrelated to that of the bulk material.⁶ However, rather more have structures clearly related to those of the bulk, although showing significant distortions. Many of the encapsulated alkali halides, with the iodides being particularly well studied,^{1–5} have structures based on the rock-salt lattice. These encapsulated crystals exhibit, when viewed down the nanotube axis, a fragment of the (0,0,1) plane of a rock-salt lattice containing either four or nine ions in cross-section depending on the diameter of the encapsulating SWNT so that there are four or nine chains of ions. Thus in the four chain (2×2) case, as shown in Figure 1, each plane consists, to within the accuracy of the experiment,² of a square arrangement of four ions with those of the same charge located at the ends of the diagonals. Although each four or nine chain structure is based on the rock-salt lattice, the inter-ionic separations are significantly distorted. Thus the inter-plane separations (b) are slightly reduced compared with

the bulk while the closest cation-anion separations (a) within each plane are appreciably dilated.^{1,2} Although there is currently significant interest in developing theoretical methods for understanding and predicting these structural distortions, the modifications of their electronic spectra from those of the bulk have received scant attention.

The most widely accepted description of the lowest energy excitation in a bulk alkali halide is that this arises as an inter-ionic charge transfer in which one of the most loosely bound halide electrons enters the lowest energy vacant s orbital on just one nearest neighbour cation.^{12–15} The discussions presented in both Sec. II B and in Secs. A and B of supplementary material¹⁶ provide strong evidence for rejecting four alternative descriptions. In the ground state of an alkali halide crystal, an anion electron occupies a spatial region in which its potential energy is lowered through its interaction with neighbouring ions, particularly its nearest cation neighbours. The dependence of this interaction on the position of an anion electron with respect to its nucleus can be expanded in a series involving spherical harmonics.^{17,18} For a crystal having either the rock-salt or cesium chloride structure, the leading non-vanishing contributions consist of a dominant term independent of any angular variables followed by one containing fourth order spherical harmonics. For the crystal at equilibrium with closest cation-anion distance R_e , the dominant potential energy contribution has a constant value^{17–19} of $-M/R_e$ when the electron is at any distance from the anion nucleus

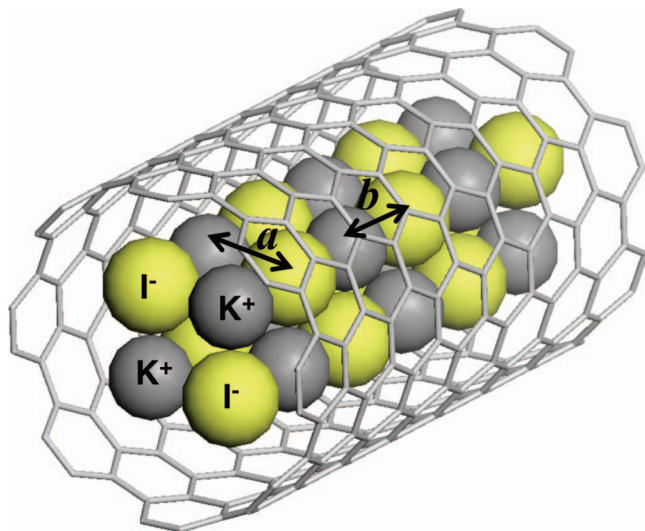


FIG. 1. A four chain (2×2) nanocrystal of potassium iodide encapsulated in a carbon nanotube.

less than R_e (M is the Madelung constant). Terms containing fourth and higher order spherical harmonics do not contribute to the energies of electrons occupying orbitals of s or p symmetry. Similar arguments^{17–19} show that a cation electron experiences a constant destabilization of M/R_e when it is at any distance from the cation nucleus less than R_e . This shows^{12–14} that, in the anion to single cation description of the excitation, interaction with the crystalline environment produces a contribution of $(2M-1)/R_e$ to the energy (ΔE_{ct}) of charge transfer. The term $-1/R_e$ arises because, after transfer to a cation, the electron interacts with one fewer anion neighbours than does a cation electron in the crystal ground state. The energy of $(2M-1)/R_e$ is the largest contribution to ΔE_{ct} , being, for the alkali halides, greater than that arising from the difference between the metal ionization potential and the halogen electron affinity.

Acceptance of the charge transfer description for bulk alkali halides would suggest that the lowest energy purely intra-crystal excitation of an encapsulated salt proceeds through the same mechanism. A study²⁰ using a Born type model, of the structures of (2×2) , (3×3) , and (4×4) nanocrystals of alkali halides, presented values for the Madelung function $M_b(x)$ which yields, for square planes of ions, the potential energy experienced by an anion electron as $-M_b(x)/b$ where $x = a/b$. Arguments identical with those used for the bulk materials show that, for the nanocrystal transition in which the electron is transferred to a neighbouring plane, the point charge electrostatic contribution to ΔE_{ct} is $(2M_b(x)-1)/b$. Comparison of this result with the corresponding expression $(2M-1)/R_e$ for the bulk shows that this contribution is smaller in the nanocrystal because $M_b(x)$ is less than the 1.74756 value of M . For (2×2) nanocrystalline KI having its experimentally observed structure, $M_b(x)$ is^{9,20} 1.51131, which lowers this contribution by slightly less than 2 eV. The natural expectation that this reduction is carried over to a redshift in ΔE_{ct} would be justified if two other significant terms were to remain essentially unchanged on passing from the bulk to the nanocrystal. The first of these is the polarization response

consisting the energies of the interaction between the dipoles induced on the ions as a consequence of two of them being replaced by neutral species. The second is the difference between the energy of interaction of a neutral alkali atom with its surroundings and that of its cation with the same surroundings after disregarding all point charge electrostatic interactions and all polarization responses.

This paper has two objectives. The first is to present a thorough investigation of the nature of the lowest energy electronic excitation in bulk alkali halides using both modern computational methods and more reliable experimental data neither of which were available to the previous investigators.^{12–15} This study not only disposes of earlier criticisms²¹ of the charge transfer description of the first excited state but also provides strong evidence that this state is composed of just a single neutral metal–neutral halogen pair as envisaged previously.^{12–14} This conclusion allows the present investigation to be confidently extended to achieving the second objective. This is to investigate the nature of the lowest energy intra-crystal electronic excitation in encapsulated nanocrystals. In particular the aim is to test the above prediction that this transition will exhibit a redshift of slightly less than 2 eV relative to that in the bulk alkali halide.

II. THEORY

A. General formulation for charge transfer descriptions

In any solid there are two fundamentally different types of excitation, those designated band to band, in which the excitation is delocalized over the entire crystal and those of the exciton type in which the excitation is localized either on only one ion or, at most, on a small number of ions immediately neighbouring the anion from which the electron was excited. For the alkali halides, the lowest energy excitation is of the second of these two types. However, there are two fundamentally different types of description of even these lowest energy excitations. In the first of these,²¹ the excitation is considered to be entirely localized on the anion and thus the states are labelled with purely atomic quantum numbers with the analysis²² relying heavily on comparison with the extensive experimental data for the iso-electronic excited states of the isolated noble gas atoms. In the second description of the excitation, one outermost anion electron is taken to be transferred into the unoccupied s orbital of one or more neighbouring cations. The purely one-centred description of the excitation will not be considered further in the main body of this paper because the evidence presented in Sec. A of supplementary material¹⁶ indicates that this description not only fails to predict the correct number of allowed optical absorptions but also, at least in its simplest form, yields qualitatively incorrect predictions for the excitation energy.

For an alkali halide, either in the bulk or as an encapsulated nanocrystal, any charge transfer description of the excitation yields its energy as^{12–14}

$$\Delta E_{ct} = A_H + I_M + \Delta E^{elst} + \Delta E^{disp} + E_{tot}^{pol}, \quad (1)$$

TABLE I. Metal ionization potentials, cation polarizabilities and neutral halogen electron affinities and polarizabilities.^{a,b,c}

Species X	Na	K	Rb	Cs	F	Cl	Br	I
$I_M A_H$ (eV)	5.139	4.341	4.177	3.894	3.400	3.616	3.365	3.066
$\alpha_C \alpha_H$ (a.u.)	1.002	5.339	9.05	15.28	3.641	14.71	20.58	33.91

^aAlkali metal ionization potentials from Moore (Ref. 40); halogen electron affinities from Smirnov (Ref. 41).

^bCation polarizabilities α_C , Na^+ , and K^+ from *ab initio* computations (Refs. 42 and 43); Rb^+ and Cs^+ from analysis (Ref. 44) of experimental molar polarizabilities.

^cNeutral halogen polarizabilities α_H , F, Cl, and Br from PNO-CI computations (Ref. 45–47); I average of two values (Ref. 48).

where I_M is the ionization potential of the neutral metal and A_H is the halogen electron affinity, defined as positive. Here ΔE^{elst} is the difference between the total electrostatic energy of the excited state of the entire crystal plus encapsulating tube and that of the ground state with all ions and neutral atoms treated as un-polarized point charges. The quantity ΔE^{disp} is the difference between the total energy arising from the dispersive attractions in the excited state and the corresponding total in the ground state. For the encapsulated crystal, ΔE^{disp} naturally includes also the difference between the dispersive attractions of the excited and ground states of the crystal to the SWNT wall. The charge transfer description of the excitation implies the existence, in agreement with experiment, of two transitions closely spaced in energy because the neutral halogen can be left not only in its ground $^2P_{3/2}$ but also in the $^2P_{1/2}$ state.¹⁴ The use of the ground state halogen electron affinity in (1) causes this to predict the lower energy of these two transitions.

For cubic crystals, the ions in the ground state reside on sites at which there are no electric fields; consequently these ions will have their usual spherical symmetry. The transfer of one anion electron to neighbouring cations introduces an inhomogeneity into the crystal in comparison with the ground state thereby creating non-vanishing electric fields and field gradients at both the remaining ions in the crystal as well as at the species directly involved in the electron transfer. The energy E_{tot}^{pol} in (1) is the total energy arising from the responses of all the species to these fields and their gradients. This total naturally includes not only the energy of interaction of each dipole induced by the non-vanishing electric field created by the ion charges but also the non-point charge electrostatic energies of interaction between the in-

duced dipoles. The acquisition of a dipole changes the charge distribution of each species, which thereby causes the energies of both the short-range overlap dependent interactions and the dispersive attractions between the species to differ from the corresponding interactions between the undistorted species. These energy changes therefore constitute contributions to E_{tot}^{pol} because they are a necessary consequence of the induced dipoles. In this work, only the leading polarization response of each atomic species, namely the electric dipole induced by the presence of non-zero electric fields, is considered.

The differences between the short-range forces in the excited and ground states of the crystal other than those entering E_{tot}^{pol} will be much smaller than the terms considered in Eq. (1). Such differences will therefore be neglected as lying outside the scope of the present investigation. The data presented in Tables I and II show that the polarizability (α_H) of a halogen and that (α_A) of its corresponding in-crystal halide ion are not very dissimilar. The coefficient [$C_6(XY)$] governing the dipole-dipole dispersive attraction between the species X and Y is closely related to the polarizabilities of the two species, this link being made explicit in the Slater-Kirkwood approximation as described in Sec. C1 of supplementary material.¹⁶ Consequently, the dispersion coefficients for the interaction of a neutral halogen and another species will not be very different from those for the interaction of the corresponding halide ion with the same other species. This shows that the differences between the dispersive attractions involving a neutral halogen and those experienced by the corresponding anion can be neglected as constituting only a minor contribution to ΔE_{ct} . However, the polarizability (α_M , see Sec. C1 of supplementary material;¹⁶ Table SIII) of a neutral alkali atom is at least 26 times greater than that (α_C , Table I) of its cation. The consequent difference between the dispersive attractions between the neutral metal and its surroundings compared with those between the cation and its surroundings will therefore produce the leading contribution (ΔE_M^{disp}) to ΔE^{disp} . The basic result (1) then becomes

$$\Delta E_{ct} = A_H - I_M + \Delta E^{elst} + \Delta E_M^{disp} + E_{tot}^{pol}. \quad (2)$$

A merit of the formulation provided by (1) and (2) is that E_{tot}^{pol} can be computed using the general utility lattice program (GULP) program²³ with the polarization of each species described using the shell model²⁴ provided that, for all pairs

TABLE II. Closest equilibrium separations (R_e) and molar polarizabilities (α_{cr}) of bulk crystals and in-crystal anion polarizabilities (a.u.)^{a,b,c}

	NaF	KF	RbF	CsF	NaCl	KCl	RbCl	NaBr	KBr	RbBr	NaI
R_e	4.355	5.018	5.280	5.682	5.287	5.904	6.172	5.599	6.180	6.446	6.056
α_{cr}	7.950	13.443	17.424	24.456	22.155	28.195	32.460	29.828	35.969	40.558	42.852
α_A	6.948	8.104	8.374	9.176	21.153	22.856	23.410	28.826	30.630	31.508	41.850
	KI	RbI	CsI(8:8)								
R_e	6.608	6.863	7.375								
α_{cr}	50.208	54.864	61.882								
α_A	44.869	45.814	46.602								

^a R_e (Ref. 28).

^b α_{cr} (Ref. 49).

^c α_A derived as $\alpha_{cr} - \alpha_C$ using the data in Table I.

of species, both the short range overlap dependent repulsive interactions and the dispersive attractions are known. Each neutral halogen polarizability, differing from that of its anion, is used to evaluate E_{tot}^{pol} .

B. Four possible charge transfer processes in bulk crystals

In a purely one-electron orbital description of the ground and excited states, an electron initially occupying the outermost p orbital of one halide ion is transferred to some linear combination of vacant s orbitals on the nearest neighbour cations. For a rock-salt structured crystal, symmetry shows that there are only three possible such final states, namely those in which the transferred electron resides respectively in an E_g , A_{1g} , or T_{1u} combination of cation s orbitals.^{15,25} The symmetries of the possible overall final states have been derived¹⁵ by taking the direct product of the each of the three above symmetries with that (T_{1u}) of the neutral halogen left after the electron transfer. Any final state, in which the transferred electron resides in either the A_{1g} or the E_g combination of s orbitals, has u symmetry. The analysis¹⁵ shows that there is at least one allowed transition both to states in which the excited electron occupies such an E_g orbital as well as to a state with this electron in such an A_{1g} orbital. However, any state with the excited electron in such a T_{1u} orbital will have g symmetry so that there are no allowed transitions to such final states. For each of these three possible final states, to be called the quadrupolar, symmetrical, and forbidden, respectively, the charge distribution, relative to that of the bulk crystal, is depicted in Figure 2. These charge distributions have a quadrupole, hexadecapole, and quadrupole, respectively, as their lowest non-vanishing multipole moment. In each of these three cases, the energy of the remaining lattice (i.e., excluding any ion whose total charge differs from that in the unexcited crystal) will be lowered as a result of the polarization of the individual ions caused by the non-vanishing electric fields created by the multipole moment of the total central structure of neutral halogen plus partially reduced cations.

A purely orbital model might be thought to preclude the existence of the excitation process in which the halide electron is transferred to just one cation neighbour, that is to an excited state of the type to be called dipolar as shown in Figure 2(a). The motivation for this observation would be that this final state does not have the correct symmetry in that it does not transform according to an irreducible representation of the O_h site symmetry of the neutral halogen. However, it is implicitly assumed, both in this observation as well as in the analysis in the preceding paragraph, that the final state can be represented by a single electronic configuration to which the lattice then responds. However, if the entire wavefunction for the final electronic state of the entire crystal in Figure 2(a), thus including the electrons on the ions in the remainder of the lattice which become polarized as a result of the charge transfer process, is called ψ_R , there is a state ψ_L which is degenerate with ψ_R . The state ψ_L differs from ψ_R only in that the halide electron is transferred to the cation lying to its left rather than, as shown in Figure 2(a), to the cation located to its right. One of the two combinations $(1/\sqrt{2})(\psi_R \pm \psi_L)$ will

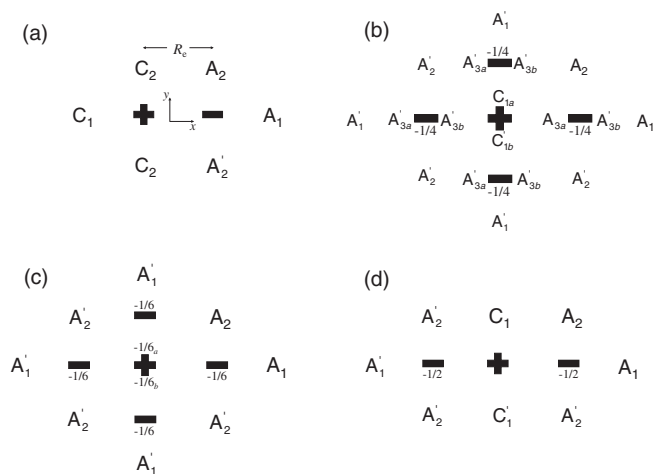


FIG. 2. Views of the xy plane for four different excited states of bulk rock-salt structured alkali halides in which one anion electron is transferred to one or more neighbouring cations. The origin of the right-handed coordinate system is located at the centre of the defect. The subscripts on the respective cation and anion labels C and A distinguish between different sets of equivalent positions. The ions with labels not carrying a prime sign are those for which the electric fields are reported in Table SI of the supplementary material. Ions in positions related by symmetry are labelled with a prime sign. The charge on each species is measured relative to that in the ground state fully ionic lattice. The neutral halogen atom is denoted by the + sign with all cations that have been either partially or wholly reduced being denoted with a - sign. The charges of partially reduced cations are indicated either above or below the - sign. (a) The dipolar excited state: The absence of a charge on the - sign denotes the metal atom carries a charge of -1 relative to that in the ground state of the fully ionic lattice. There are two more ions A'_2 located at $(R_e/2, 0, \pm R_e)$. (b) The quadrupolar excited state: The symbols A'_{3a} and A'_{3b} denote anions located at a distance R_e respectively above and below the partially reduced cations, so that ion A'_{3a} is located at $(R_e, 0, R_e)$. (c) The symmetrical excited state: The symbols $-1/6_a$ and $-1/6_b$ denote partially reduced cations carrying a charge of $-1/6$ located at a distance R_e respectively above and below the neutral halogen. There are two more ions A'_1 located at $(0, 0, \pm 2R_e)$ and eight more ions A'_2 located at $(\pm R_e, 0, \pm R_e)$ and $(0, \pm R_e, \pm R_e)$ taking all possible combinations of the \pm sign. (d) The forbidden excited state. There are two more ions C'_1 located at $(0, 0, \pm R_e)$. The ion A_4 is located above C_1 at $(0, R_e, R_e)$ with symmetry related ions A'_4 at $(0, R_e, -R_e)$ and $(0, -R_e, \pm R_e)$.

have T_{1u} symmetry so that the transition to this state from the ground state will be allowed. The correct energy will be calculated considering only ψ_R provided that the matrix element linking this with ψ_L is small. For a macroscopic solid, this matrix element should be expected to be vanishingly small because the electronic Hamiltonian contains only one-body and two-body terms while the two wavefunctions each consist of a sum of products of a large number of one-electron orbitals with each orbital in ψ_R having an overlap with the corresponding function in ψ_L which is less than unity. Thus the matrix element will contain products of a very large number of overlap integrals causing each product and hence the entire matrix elements to be vanishingly small. In this situation, it has been pointed out,²⁶ by invoking Ocam's Razor, that the correct states to use are the symmetry breaking ψ_L and ψ_R rather than the symmetry adapted linear combinations $(1/\sqrt{2})(\psi_R \pm \psi_L)$. These symmetry broken states are analogous to those of N_2^+ and O_2^+ produced^{26,27} by ionization of a $1s$ core electron from N_2 and O_2 neutral molecules where the $1s$ hole has an equal probability of being localized on one

of the two atoms rather than being delocalized over the entire molecule.²⁷

The use of the combination $A_H - I_M$ in (2) for the quadrupolar, symmetric and forbidden final states will provide a very good approximation even though the transferred electron is delocalized over more than one cation because the matrix elements between different cation wavefunctions will be small. Clearly there is no such approximation in using the combination $A_H - I_M$ for the dipolar final state.

The contribution (ΔE_M^{disp}) to ΔE^{disp} would be expected to be similar for the four different final states shown in Figure 2. Consequently the differences between these four excitation energies will be essentially determined by differences in the lattice polarization term E_{tot}^{pol} . The fields generated by point dipoles, quadrupoles, and hexadecapoles decrease with increasing distance as R^{-3} , R^{-4} , and R^{-6} , respectively. It would therefore be expected, provided that the description of the defect as a point multipole is not grossly in error, that the fields created by the dipolar defect would be greater than those arising from the three defects having only higher non-vanishing multipoles. Each multipole will create an electric field at any other ion X thereby producing an energy $-(1/2)\alpha_X|F_X^2|$ additional to that of the ion in the crystal ground state. Here $|F_X^2|$ is the square magnitude of the electric field at X created by the multipolar defect. However, use of the point multipole description of the defect must be questionable for an ion located at a distance R_e from any species in the central multipole. The field at each such ion having a central multipole species as a nearest neighbour was evaluated, as detailed in Sec. B of supplementary material,¹⁶ by summing the fields created by each individual species constituting the multipole. The total polarization energy arising from all these closest ions was then derived by summing the quantities $-(1/2)\alpha_X|F_X^2|$ over all of these closest bulk ions. Since all the lengths in this calculations are proportional to R_e , with the field generated by each point charge being proportional to R_e^{-2} , the polarization energies arising from each of these four defects are proportional to R_e^{-4} . These four polarization energies are distinguished by having different coefficients multiplying the individual ion polarizabilities. The resulting expressions for these close neighbour contributions to E_{tot}^{pol} are presented in the first numerical column of Table III (for the forbidden defect the four anions located at a distance $\sqrt{2}R_e$ from the neutral halogen were also included as close neighbours). The symmetry of the dipolar final state enables the result to be expressed in terms of the molar polarizability $\alpha_{cr} = \alpha_C + \alpha_A$. Ions located at distances greater than R_e (and $\sqrt{2}R_e$ for the forbidden state) from any ion in the multipole were treated, as described in Sec. B of supplementary material,¹⁶ as a continuous distribution of polarizable material having a density α_{cr}/V_m with V_m the molar volume. The resulting contributions to the polarization energy, again proportional to R_e^{-4} , are presented in the second numerical column of Table III. The contributions of the close neighbour ions are at least four times greater than those yielded by the continuum description of the more distant ions. Furthermore the closest neighbour contribution in the dipolar excited state (Figure 2(a)) is much greater than that in the quadrupolar (Figure 2(b)) case and is, furthermore, at least 21 times greater

than the energy in the symmetrical (Figure 2(c)) state. The contribution from the more distant ions in the symmetric case is therefore negligible and hence not reported in Table III. The total polarization energies E_{tot}^{pol} reported in the last column of Table III were derived by summing the contributions in the two preceding columns. Since, for the dipolar excited state, E_{tot}^{pol} (negative) is so much greater in magnitude than for either the quadrupolar or symmetric cases, it can be concluded that neither of the latter two charge distributions is present in the first excited state. This conclusion is strengthened by noting that the coefficient (1.724) of the anion polarizability for the dipolar state is 7 times greater than that for the quadrupolar state; anion polarizabilities being significantly larger than those of cations. Furthermore, since not only is the magnitude of E_{tot}^{pol} in the dipolar state significantly greater than that in the forbidden state (Figure 2(d)) but also the transition to this state is forbidden, it can be concluded that the first excited state contains the dipolar charge distribution shown in Figure 2(a) as originally envisaged in the 1930s.¹²⁻¹⁴ The magnitude of E_{tot}^{pol} predicted for the dipolar state is so much greater than that in the other three excited states, that the conclusion that the dipolar state lies lowest in energy would not be altered by including in the calculations the interactions between the dipoles induced on the individual ions. Hence, in all the following calculations, the excited state will be taken to have the dipolar structure.

For the dipolar excitation, the point charge electrostatic contribution (ΔE^{elst}) reduces, for bulk crystals having either the rock-salt or cesium chloride structures, to $(2M - 1)/R_e$ for the reasons presented in the introduction. In this case the result (2) becomes

$$\Delta E_{ct} = A_H - I_M + (2M - 1)/R_e + \Delta E_M^{disp} + E_{tot}^{pol}. \quad (3)$$

For bulk crystals, this is key relation upon which all the numerical computations presented in this paper are based. These computations automatically include in E_{tot}^{pol} the interactions between the dipoles induced on the individual mononuclear species.

An approximate analytic expression for E_{tot}^{pol} was presented many years ago as detailed in Sec. IV B. The predictions from this approximate result can be compared with the significantly more accurate values computed from the result (3) using the GULP program.

C. Dipolar description of intra-crystal excitations in encapsulated crystals

For an encapsulated alkali halide in which each plane is (2×2) in cross-section containing four ions, there will be two intra-crystal charge transfer transitions to final states containing an alkali atom immediately neighbouring the neutral halogen resulting from the electron transfer. There are two such final states, even after disregarding spin-orbit coupling in the neutral halogen, because, as depicted in Figure 3, the neutral metal-halogen pair can either be orientated perpendicular to the nanotube axis with the pair lying entirely in one plane or it can be aligned parallel to the axis with the neutral atoms occupying adjacent planes. The arguments, which yield

TABLE III. Approximate formulae for the lattice polarization energies for four possible excited states of rock-salt structured crystals (a.u.).^{a,b}

Excited state	Close neighbours	More distant	Total
Dipolar	$-1.367\alpha_{cr}$	$-0.357\alpha_{cr}$	$-1.724\alpha_{cr}$
Quadrupolar	$-(0.418\alpha_C + 0.214\alpha_A)$	$-0.030\alpha_{cr}$	$-(0.448\alpha_C + 0.244\alpha_A)$
Symmetrical	$-0.082\alpha_{cr}$		$-0.082\alpha_{cr}$
Forbidden	$-(0.836\alpha_C + 0.622\alpha_A)$	$-0.121\alpha_{cr}$	$-(0.957\alpha_C + 0.743\alpha_A)$

^a E_{tot}^{pol} in a.u. given by multiplying the tabulated result by R_e^{-4} with R_e in a.u.

^b Close neighbours are those at a distance R_e from any species in the defect with further anions located at $\sqrt{2}R_e$ from the neutral halogen being also included in the forbidden case.

the result (2) for the bulk crystals, show that the energies of the intra-crystal charge transfer transitions in the encapsulated alkali halide nanocrystals can be predicted from

$$\Delta E_{ct}(f) = A_H - I_M + \Delta E^{elst}(f) + \Delta E_M^{disp}(f) + E_{tot}^{pol}(f). \quad (4)$$

Here the parameter f , which can take either of the values \perp or \parallel , distinguishes between the two possible orientations of the neutral pair with respect to the nanotube axis. The energy $\Delta E^{elst}(f)$ is the difference between the point charge electrostatic energies of the final and initial states in the absence of the polarization response. The result (4) is valid even if the individual planes of four ions are not square but are diamond in shape as predicted by the computations⁹ for the ground state structures. In this case, $\Delta E^{elst}(f)$ has to be computed with the GULP program after removing the shell model description of

the ion polarizabilities because, in contrast to the bulk crystals, there is, in general, no analytic result.

Although the computations predict diamond shaped planes, the deviations of the inter-ionic angles from 90° are smaller than the errors in the experiments² from which it was deduced that the four ion planes are square. In the latter case, $\Delta E^{elst}(f)$ reduces to $2M_b(x)/b - 1/d(f)$, when (4) becomes

$$\Delta E_{ct}(f) = A_H - I_M + 2M_b(x)/b - 1/d(f) + \Delta E_M^{disp}(f) + E_{tot}^{pol}(f) \quad (5)$$

with the distance $d(f)$ taking the value a for $f = \perp$ but is b for $f = \parallel$.

III. METHODS FOR THE DIPOLAR DESCRIPTION

The metal ionization potentials and halogen electron affinities required to calculate the excitation energies in both the bulk salts and the encapsulated nanocrystals are presented in Table I. For the bulk crystals, the equilibrium closest cation–anion separations²⁸ R_e used throughout are presented in Table II. The computations with the GULP program require the values of the individual ion polarizabilities as well as those of the neutral halogen atoms, all these quantities being presented in Tables I and II.

Evaluation of the dispersive contributions ΔE_M^{disp} and $\Delta E^{elst}(f)$ requires values for the coefficients governing both the dipole-dipole and dipole-quadrupole dispersive attractions as well as for the parameters controlling the damping^{29,30} of these attractions for separations at which overlap of wavefunctions of the interacting species is not negligible. For the intra-crystal interactions, the required numerical values, presented in Sec. C1 of supplementary material,¹⁶ were derived using the previously described methods of proven reliability.^{18,31–34} For the encapsulated crystals, the coefficients governing the dispersive attractions between the carbon atoms and the ions have already been presented⁹ while those (see Sec. C1, Table SVI of supplementary material¹⁶) for the interactions between the carbon atoms and neutral alkalis were calculated using the same methods.³⁵ For both the carbon atoms and the neutral halogens, the dispersive attractions were derived as their spherical averages. Both the Axilrod-Teller interactions and higher order dispersive attractions were omitted since these will be much smaller than the dispersion terms included.

The GULP computation of the total polarization energy E_{tot}^{pol} requires, in addition to the polarizability of each

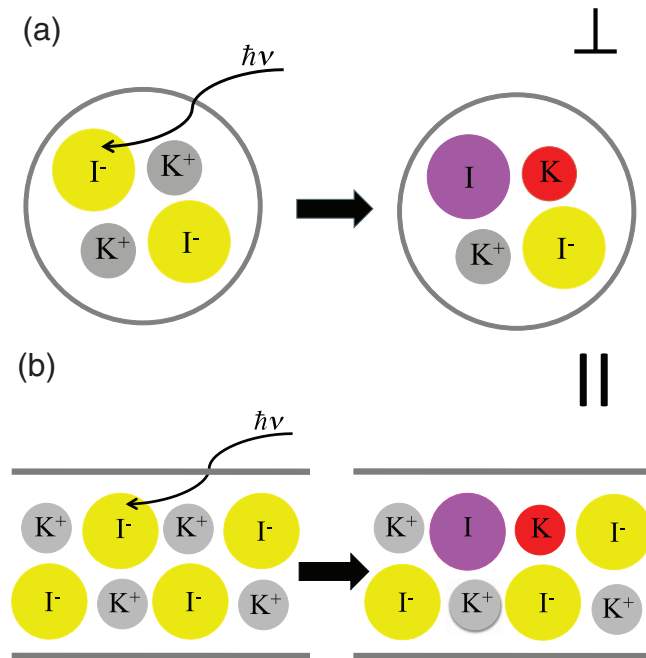


FIG. 3. Schematic diagrams of the lowest energy intra-ionic excitations of a four chain alkali halide encapsulated in a carbon nanotube. A photon is absorbed by an anion (yellow) leaving a neutral halogen (violet) with an electron transferred to a cation (gray), which becomes reduced to an atom (red) of the normal metal. (a) The transition to the “perpendicular” state with the transferred electron remaining in the same four atom plane. (b) The transition to the “parallel” state with the excited electron transferred to the neighbouring four atom plane.

TABLE IV. Bulk crystal lowest excitation energies computed using Eq. (3) and the GULP program (eV).^a

	KCl	RbCl	KBr	RbBr	KI	RbI	CsI(8:8)
$A_H - I_M$	-0.73	-0.56	-0.98	-0.81	-1.27	-1.11	-0.83
$(2M-1)/R_e$	11.50	11.00	10.99	10.53	10.27	9.89	9.32
ΔE_M^{disp}	-1.51	-1.45	-1.49	-1.48	-1.46	-1.40	-1.83
E_{tot}^{pol}	-1.55	-1.66	-1.58	-1.58	-1.96	-1.66	-1.21
ΔE_{ct} comp.	7.71	7.89	6.94	6.66	5.58	5.73	5.45
ΔE_{ct} expt.	7.60	7.40	6.58	6.43	5.63	5.55	5.69 ^b

^aAll experimental results from Table VIII (p. 242) of Ref. 13 except for CsI.

^bTaken from Figure 3 of Ref. 50.

mononuclear species, the shell charges and spring constants entering the shell model. For the SWNT carbon atoms, these parameters have already been reported³⁵ while, for the cations and metal atoms, the derivation of the two latter quantities is presented in Sec. C1 of supplementary material.¹⁶ For the anions, further experimental dielectric data are needed to determine the shell charges and spring constants. The derivation of the necessary parameters, using methods^{35,36} of established reliability, is described in Sec. C1 of supplementary material.¹⁶ The GULP computations require, in addition to the dispersive attractions, the short-range overlap dependent repulsive interactions between all pairs of species. Those for the purely intra-ionic interactions have either been presented previously, as for RbCl³⁶ and the iodides,³⁷ or were computed by the same methods based on using the in-house RELCRION program as described in Sec. C2 of supplementary material.¹⁶ The short-range interactions between the ions and SWNT carbon atoms have already been computed.⁹ The predicted excitation energies naturally depend on the nuclear positions. The shell model computations of the polarization responses therefore needed to be performed using a predicted equilibrium nuclear geometry closely reproducing experiment. The full details are presented in Sec. C3 of supplementary material.¹⁶

IV. BULK CRYSTAL PREDICTIONS FOR THE DIPOLAR DESCRIPTION

A. Fully computational approach

The availability of suitable inter-ionic potentials allows the lowest excitation energy in seven bulk alkali halides to be predicted using the GULP program from the full theory based on Eq. (3) thereby including, through the term E_{tot}^{pol} , the entire polarization response. These results both constitute a fundamental test of the charge transfer description of the excitation as well as providing a benchmark against which the reliability of calculations based on the approximate theory presented in Sec. IV B can be assessed.

The bulk alkali halides considered in Table IV all have the six-fold co-ordinated (6:6) rock-salt structure excepting CsI, which has the eight fold (8:8) coordinated CsCl structure. All the predictions for their excitation energies agree well with experiment. This constitutes good evidence that the excitation process consists of the transfer of one halide electron to just a single neighbouring cation. The results in Table IV show that, while the point charge Madelung term makes the largest contribution to ΔE_{ct} , each of the three

other terms constitutes a significant factor acting to reduce the excitation energy. This disposes of one of three previous criticisms²¹ of the charge transfer description, namely the comment that use of just terms $A_H - I_M$ and $(2M-1)/R_e$ failed to reproduce experiment. The well-founded theory underlying the computations of E_{tot}^{pol} and ΔE_M^{disp} coupled with the good agreement between the calculated and experimental values of ΔE_{ct} disposes of the two further criticisms. The first of these²¹ was that the overestimation of ΔE_{ct} arising by considering only the first three terms of (1) or (2) could only be rectified by introducing questionable assumptions and second was that the metal dependent terms could not be properly evaluated.

Increase of the polarizabilities of the constituent ions enhances the dispersion coefficients thereby acting to augment the magnitudes of the ΔE_M^{disp} . Furthermore, increasing ionic polarizabilities also act to enhance the magnitudes of E_{tot}^{pol} . However, crystals with larger ion polarizabilities have larger R_e values, which therefore act to reduce the magnitudes of both ΔE_M^{disp} and E_{tot}^{pol} in opposition to ionic polarizability effect. This explains why these two contributions to ΔE_{ct} are not markedly dependent on crystal for the rock-salt structured materials. In particular all six values of ΔE_M^{disp} differ from -1.47 eV by no more than a mere 0.07 eV.

The values (first line of Table V) of the lattice polarization energies calculated for the dipolar final states by using the approximate expression presented in Table III are smaller in magnitude than the E_{tot}^{pol} values (Table IV) computed using the GULP program because the latter also include the polarization energies of the neutral metal and halogen atoms. However, the polarization energy, denoted E_{polcr}^{GULP} , of the lattice alone excluding those of the neutral atoms has been computed using the GULP program as described in Sec. IV B. The results, reported in the first line of Table VI show that the magnitude of E_{polcr}^{GULP} is overestimated by the approximate (Table III) expression. This overestimation arises because

TABLE V. Approximate lattice polarization energies predicted for four possible final states (eV).^a

State	KCl	RbCl	KBr	RbBr	KI	RbI
Dipolar	-1.09	-1.04	-1.15	-1.10	-1.24	-1.16
Quadrupolar	-0.18	-0.18	-0.18	-0.19	-0.19	-0.19
Symmetric	-0.04	-0.04	-0.05	-0.04	-0.05	-0.05
Forbidden	-0.49	-0.49	-0.59	-0.61	-0.60	-0.61

^aCalculated from the formulae in the last column of Table III using R_e values and polarizabilities in Tables I and II.

TABLE VI. Analysis of bulk polarization energies (eV).^{a,b}

	KCl	RbCl	KBr	RbBr	KI	RbI	CsI
E_{polcr}^{GULP}	-0.83	-0.91	-0.92	-0.95	-0.97	-0.93	-0.93
E_{polM}^{GULP}	-0.50	-0.38	-0.39	-0.45	-0.42	-0.39	-0.02
E_{polH}^{GULP}	-0.10	-0.09	-0.12	-0.14	-0.12	-0.11	-0.08
E_{polS}^{GULP}	-1.43	-1.38	-1.42	-1.54	-1.51	-1.43	-1.03
E_{pol}^{anal}	-1.45	-1.37	-1.55	-1.46	-1.69	-1.57	

^aGULP predictions computed as described in the text.

^b E_{pol}^{anal} calculated as the sum of the polarization energies of the crystal (Eq. (8)) and the neutral halogen (Eq. (9)).

the interactions between the induced dipoles were neglected in the latter calculations. However, the result that the overestimations of the magnitudes of E_{polcr}^{GULP} by the approximate expression do not exceed 30% of the accurate (Table IV) values shows that the predicted magnitudes of this quantity for the quadrupolar, symmetrical, and forbidden final states will similarly be overestimated. However, the magnitudes of all three of these quantities (Table V) are so small that ΔE_{ct} would be seriously underestimated, by at least 1 eV, compared with experiment if the accurate values of E_{tot}^{pol} in Table IV for the dipolar final state were to be replaced by those predicted for any of the other three final states described in Sec. II B. This result coupled with the variational arguments provides conclusive evidence that the excitation process not only involves anion to cation electron transfer but also that this transfer is to only a single cation thereby generating the dipolar final state as envisaged in the publications¹²⁻¹⁴ from the 1930s.

For seven pairs of crystals, Table VII presents an analysis of the differences ($\Delta[\Delta E_{ct}]$) in the excitation energies as derived from the results (Table IV) of the GULP computations. The R_e value in the first member of each pair is smaller than that of the second so that the change $\Delta[(2M-1)/R_e]$ in the point charge Madelung contribution is always positive. Since the contributions ΔE_M^{disp} in all the six rock-salt structured crystals are so similar (Table IV), the differences in these terms hardly contribute to any of the seven differences $\Delta[\Delta E_{ct}]$ considered in Table VII. The results for the first four pairs reveal the effect of increasing anion size keeping the cation fixed. The increase of anion polarizability with increasing anion size more than outweighs the effect of increased R_e

TABLE VII. Analysis of differences of bulk crystal excitation energies computed using the GULP program (eV).^a

Pair	KCl	RbCl	KCl	RbCl	KI	KBr	KCl
	KI	RbI	KBr	RbBr	RbI	RbBr	RbCl
$\Delta(A_H - I_M)$	0.54	0.55	0.25	0.25	-0.16	-0.17	-0.17
$\Delta[(2M-1)/R_e]$	1.23	1.11	0.51	0.47	0.38	0.46	0.50
$\Delta(\Delta E_M^{disp})$	-0.05	-0.05	-0.03	0.03	-0.06	-0.01	-0.06
$\Delta(E_{tot}^{pol})$	0.39	0.56	0.01	0.48	-0.30	0.0	-0.47
$\Delta(\Delta E_{ct})$ comp	2.11	2.17	0.74	1.23	-0.14	0.28	-0.20
$\Delta(\Delta E_{ct})$ expt.	1.97	1.85	1.02	0.97	-0.15	0.15	0.20

^aChange ΔP in excitation energy contribution P equals value of P for crystal in top line minus the value for the crystal in the second line.

causing E_{tot}^{pol} to be of smaller magnitude for the crystal with the smaller anion. This causes ΔE_{tot}^{pol} to be positive thereby re-reinforcing the tendency of the point charge Madelung contribution to increase $\Delta[\Delta E_{ct}]$. This contrasts the situation with the last three pairs considered in Table VII examining the effect of increasing the cation size keeping the anion constant. The cation polarizabilities are significantly smaller than those of the anions, which cause the effect of increasing R_e to more than offset the increased polarizability of the heavier cation in each pair. This causes E_{tot}^{pol} to be greater in magnitude for the crystal with the lighter cation. Consequently, the differences $\Delta[\Delta E_{ct}]$ are small for these pairs as the two largest contributors $\Delta[(2M-1)/R_e]$ and ΔE_{tot}^{pol} have opposite signs.

B. Simplified analytic description

The GULP computations could only be performed for those systems for which the potentials and anion wavefunctions computed using the RELCRION program were available. The evaluation of the dispersive attractions requires the anion wavefunctions to derive the anion dispersion damping parameters. The approximate theory presented in this subsection is of interest because it enables the excitation energies to be predicted for other alkali halides for which inter-ionic potentials have not so far been computed. In particular, it is important to show that the charge transfer description of the excitation does not experience any catastrophic breakdown when applied to other alkali halides, particularly fluorides since these do not appear amongst the seven crystals investigated using GULP computations.

The systems not studied computationally can be investigated by using the theory^{13,14} of the dipolar excitation presented in the 1930s. This theory, which contains essentially the same physics as that described by Eq. (3), expresses ΔE_{ct} as

$$\Delta E_{ct} = A_H - I_M + (2M - 1)/R_e + E_{cr}^{pol} + \Delta E_H + \Delta E_M. \quad (6)$$

Here E_{cr}^{pol} is the energy arising from the polarization of the lattice induced by the neutral pair generated by the charge transfer. The energy E_{cr}^{pol} does not include any of the contributions arising from polarization of either of the two neutral species that result from the charge transfer excitation. The quantity ΔE_H is, disregarding the point charge electrostatic effect included in the $(2M-1)/R_e$ term, the difference between the interaction with the remaining lattice of a neutral halogen and a halide ion. The last term in (6), ΔE_M , is similarly the difference between the interaction with the remaining crystal of the neutral metal and that of the cation precursor of the metal. The two largest contributions to ΔE_M are the polarization energy (E_M^{pol}) of the metal induced by the electric field created by its neutral halogen neighbour and the greater dispersive attraction of the metal to the remaining lattice when compared with the attraction experienced by the cation. After neglecting the differences between the short-range interactions of the metal and cation with the remaining lattice, expected to be much smaller as discussed in Sec. II, it is seen that

$$\Delta E_M = \Delta E_M^{disp} + E_M^{pol}. \quad (7)$$

If the differences, expected to be small, between the short-range interactions involving the neutral halogen and its anion are neglected, the sum of the three terms E_{cr}^{pol} , ΔE_H , and E_M^{pol} constitutes the total polarization contribution to ΔE_{ct} in the approach yielding (6). This sum is thus describing the same physics as the term in E_{tot}^{pol} (3) although the later will be more accurate as its computation includes the interactions between the different induced dipoles. These are only partially included in (6) because there the three contributions E_{cr}^{pol} , ΔE_H , and E_M^{pol} are taken to be additive.

For the rock-salt structure E_{cr}^{pol} , evaluated in the point dipole approximation, has been reported to be³⁸

$$E_{cr}^{pol} = -2.027\alpha_{cr}/R_e^4. \quad (8)$$

The alternative approximate result (Table III) derived in this paper is similar to (8) differing only in the replacement of -2.027 by -1.724 . For the alkali halides, the predictions (Table V) are only 0.2 eV smaller in magnitude than those derived from (8). The contribution ΔE_H was interpreted solely as the polarization response, again treated as a point dipole, of a neutral halogen of polarizability α_H and thus given by¹³

$$\Delta E_H = -(1/2)\alpha_H/R_e^4. \quad (9)$$

The only contribution in (6) that cannot be evaluated analytically from readily available experimental data is ΔE_M . It was, therefore, this term, which presented the greatest difficulty in previous applications of (6). Thus in one work,³⁹ ΔE_M was taken to be constant with a value of about -1 eV for all alkali halides whereas in another¹³ it was estimated as the geometric mean of the sublimation energies of the bulk alkali metal and bulk ionic crystal. In a third investigation,¹⁴ a value of -1.6 eV was deduced for NaCl by substituting the experimental value of ΔE_{ct} into (6) and then using the relations (8) and (9). The results (Table IV) computed using the GULP program show that, for the rock-salt structured crystals, the dispersion contribution (ΔE_M^{disp}) to ΔE_M are very similar deviating by no more than 0.07 eV from the average value of -1.47 eV. The result that this contribution, although only one of the two terms of ΔE_M , is somewhat similar to previous^{13,14,39} more empirical evaluations of ΔE_M is evidence for the correctness of their conclusion^{13,39} that the interaction between the metal atom and the remaining lattice cannot be neglected. Considering only the ΔE_M^{disp} contribution to ΔE_M and taking this to be constant at the average (-1.47 eV) of the values we have calculated for the six rock-salt structured crystals considered in Table IV enables ΔE_{ct} for all the rock-salt structured alkali halides to be predicted from (6), (8), and (9).

For the six rock-salt structured crystals considered in Table IV, the excitation energies (ΔE_{ct} , Table VIII) predicted from the analytic formula (6), implemented as just described, agree well with both experiment and those yielded by the GULP computations. Furthermore, for the materials not considered in Table IV, the discrepancies between experiment and the predictions (Table VIII) thus derived from (6) are no greater than those for the former six crystals. This shows that the materials not considered in Table IV do not provide any evidence against the dipolar charge transfer description of the first excited state.

TABLE VIII. Bulk lowest excitation energies predicted using Eqs. (6), (8), and (9) (eV).^{a,b,c}

	KCl	RbCl	KBr	RbBr	KI	RbI	
E_{cr}^{pol}	-1.28	-1.23	-1.36	-1.30	-1.45	-1.36	
ΔE_H	-0.17	-0.14	-0.19	-0.16	-0.24	-0.21	
ΔE_{ct} comp.	7.82	7.62	7.06	6.78	5.84	5.81	
ΔE_{ct} expt.	7.60	7.40	6.58	6.43	5.63	5.55	
	NaF	KF	RbF	CsF	NaCl	NaBr	NaI
E_{cr}^{pol}	-1.22	-1.17	-1.24	-1.29	-1.56	-1.67	-1.76
ΔE_H	-0.14	-0.08	-0.06	-0.05	-0.26	-0.28	-0.34
ΔE_{ct} comp.	11.02	9.87	9.28	8.64	8.03	6.92	5.57
ΔE_{ct} expt.	10.70	9.98	9.21	9.19	7.8	6.50	5.39

^aSee footnote a to Table III for first six crystals, NaBr and NaI, fluoride values taken from the experimental spectra presented in Ref. 22, NaCl value from Ref. 51.

^b E_M^{pol} neglected.

^cFor first six crystals full calculation of ΔE_M^{disp} , for last seven crystals ΔE_M^{disp} approximated as constant at -1.47 eV, see text.

The good agreement between the analytic predictions and experiment (Table VIII) might seem surprising in view of the neglect, in the present implementation of (6), of the contribution E_M^{pol} arising from the static dipole polarization of the metal atom. The significance of both this contribution and the accuracy of the point dipole expressions (8) and (9) can be probed by computing each of these three terms with the GULP program. This was achieved by performing, for each crystal, three separate GULP computations in which only the metal atom, all the ions and just the neutral halogen were polarizable. Subtraction of both the point charge Madelung energy (ΔE_{elst}) and ΔE_M^{disp} from the computed values of ΔE_{ct} yields the GULP predictions, denoted E_{polM}^{GULP} , E_{polcr}^{GULP} , and E_{polH}^{GULP} , for the separate polarization responses of the metal atom, ionic lattice, and neutral halogen, respectively. The results, presented in Table VI, show that the sum of these three polarizations (E_{polS}^{GULP}) underestimates the full polarization energy (E_{tot}^{pol}) presented in the fourth numerical row of Table IV. However, it is only for KI that the discrepancy exceeds 0.18 eV. The computed results for E_{polM}^{GULP} show that E_M^{pol} cannot be reliably evaluated as the point dipole response $-(1/2)\alpha_M/R_e^4$, analogous to (9) for ΔE_H . Thus, using the metal atom polarizabilities (see Table SIII of the supplementary material¹⁶), this expression predicts E_{polM}^{GULP} to be -3.28 eV, -2.99 eV, and -2.09 eV for KCl, RbCl, and KI, respectively. These values are at least four times greater in magnitude than the reliable computed results presented in Table VI. Similarly the predictions (E_{cr}^{pol} , Table VIII) of the crystal polarization energies provided by (9) are 0.4 eV -0.5 eV greater in magnitude than those (E_{polcr}^{GULP} , Table VI) computed using the GULP program. The magnitudes of the analytic predictions of the halogen polarization energies (ΔE_H) are also roughly twice the small (~ 0.1 eV) values derived from the GULP computations. The analytic formulae overestimate the magnitudes of all the polarization responses compared with the more reliable GULP predictions because the former do not take account of the damping of the polarizations caused by the differences between the short-range repulsions of polarized and unpolarized species. These effects

are included in the GULP computations through the interactions between different shells.

The above comparison of the analytic and GULP polarizations shows that the closeness of the agreement between the present analytic (Eq. (6)) and the computed predictions of the total excitation energies (ΔE_{ct}) is slightly fortuitous. Thus Eq. (6) overestimates the magnitude of the sum of the crystal and halogen polarization energies by 0.4 eV–0.5 eV, which is precisely the range of values predicted by the GULP computations for the metal polarization energies neglected in (6). However, the agreement between experiment and the predictions of (6) for the systems not studied using the GULP program are no worse than those for the six studied computationally. This result coupled with the fact that the discrepancies in the individual polarization components do not exceed 0.5 eV shows that the systems not studied computationally do not provide any evidence to contradict the conclusion that the first excited state has the dipolar structure involving electron transfer to just a single cation as shown in Figure 2(a).

V. INTRA-CRYSTAL EXCITATIONS IN ENCAPSULATED POTASSIUM IODIDE

A KI nanocrystal, effectively infinite in length along the SWNT axis with each plane consisting of four ions has been encapsulated² in a SWNT whose experimental radius was, to within experimental error, equal to that of a (16,0) tube. The distance (a) between two closest ions of opposite charge in any one four-ion plane was deduced² from electron microscopy to be 3.98 Å, there being no experimental evidence that these planes are not square. The interplane distance (b) was measured in the same experiments to be 3.50 Å. For the case in which the four ion planes are square, the final state (f) with the anion electron transferred to a cation in a neighbouring plane will be designated Sq|| while that with a purely intra-planar excitation being labelled Sq⊥. The corresponding final states with diamond shaped planes will be denoted Di|| and Di⊥, respectively. The computations for the square planes were performed using the above experimental values of a and b . There is currently no experimental data on the geometry of the diamond shaped planes predicted as the optimal structure by the computations.⁹ The a and b values of 3.97 Å and 3.54 Å predicted by these computations will therefore be used to define the geometry.

The predictions for the excitation energies and their components derived using (4) or (5) are compared in Table IX with those computed for bulk KI. The total excitation energies ($\Delta E_{ct}(f)$) predicted for all of the four possible excited states are lower than that in the bulk material. For the excitations to the parallel (||) final states, the energy decreases of 1.16 eV and 1.45 eV are significant. This confirms the suggestion of a redshifted excitation motivated by considering just the electrostatic contribution in the case of the Sq|| final state as discussed in the introduction. For this case $\Delta E^{elst}(\parallel)$ is reduced by 1.903 eV (10.275 eV–8.372 eV) compared with the bulk. The analytic approximation (47) of Ref. 20 predicts that $M_b(x)$ is 1.5113 when x has the 1.137 (=3.98/3.50) value for square four ion planes thus yielding a result of 8.321 eV

for $\Delta E^{elst}(\parallel)$. The very close agreement of this result with the exact value of 8.372 eV justifies using the approximation²⁰ in the motivation of the present investigation. For the Di|| final state the electrostatic contribution of 2.14 eV to the redshift is similar to that of 1.90 eV for the Sq|| case.

For all four excitations, the change in the electrostatic contribution ($\Delta E^{elst}(f)$) has a greater magnitude than that in either of the other two terms ($\Delta E_M^{disp}(f)$ and $E^{pol}(f)$) entering $\Delta E_{ct}(f)$ in Eq. (5). However, for the transition to either of the perpendicular (⊥) excited states, the electrostatic contribution to the redshift is reduced by $(1/b) - (1/a)$ a.u. compared with that for the transition to the || state having the same nuclear geometry. These differences arise, as demonstrated by both the relations (4) and (5), because the electron transferred to the cation interacts with one fewer anion neighbours than does a cation electron in the ground state, the oxidized anion being further from the cation for ⊥ excited states. For the final states having respectively the square and diamond shaped (2×2) planes, the redshift reductions (= $(1/b) - (1/a)$) in $\Delta E^{elst}(f)$ are 0.50 eV and 0.43 eV.

The redshifts in $\Delta E^{elst}(f)$ might not be fully reflected in the reduction of $\Delta E_{ct}(f)$ because, on passing from the bulk to the nanocrystal, the two remaining contributions ($E^{pol}(f)$ and $\Delta E_M^{disp}(f)$) could, in principle, change significantly. However, a combination of two factors causes the dispersion contributions ($\Delta E_M^{disp}(f)$) to be very similar for all four final states of the nanocrystals. Thus, first, each term ($\Delta E_M^{disp}(f)$) is a simple sum of the contributions from the interactions of either the metal atom or its cation with all the other species present while, second, the inter-species separations in the states having the diamond shaped planes are very similar to those for the states with square planes. The result that the magnitude of $\Delta E_M^{disp}(f)$ is slightly greater for the encapsulated material than for the bulk crystal shows that the interactions with the nanotube carbon atoms must be significant. The presence of these interactions in the encapsulated material more than compensates for the absence, compared with the bulk crystal, of some of the dispersive attractions between the metal atom and ions located at greater distances. However, the near equality between the dispersion contributions in the bulk crystal with those for the encapsulated materials might be specific to the case of KI.

The data presented in Table IX show that the polarization contribution ($E^{pol}(f)$) to $\Delta E_{ct}(f)$ is significantly reduced

TABLE IX. Intra-crystal excitation energies for encapsulated (2×2) KI (eV).^a

Excitation, f	$\Delta E^{elst}(f)$	$\Delta E_M^{disp}(f)$	$E^{pol}(f)$	Sum ^b	$\Delta E_{ct}(f)$
Bulk	10.27	−1.46	−1.96	6.85	5.58
Sq	8.37	−1.51	−1.17	5.70	4.42
Sq⊥	8.87	−1.50	−0.73	6.64	5.36
Di	8.13	−1.59	−1.14	5.40	4.13
Di⊥	8.58	−1.59	−0.38	6.61	5.34

^a $\Delta E^{elst}(f)$ for the nanocrystals computed using the GULP program. For the square || and square ⊥ crystals, the finite analytic approximation (47) of Ref. 20 predicts respective values of 8.42 eV and 8.82 eV.

^b Sum is the total of the previous three columns, that is $\Delta E_{ct}(f)$ without the contribution $A_H - I_M$.

in the encapsulated material compared with that for the bulk crystal. This explains why the redshifts in $\Delta E_{ct}(f)$ for the excitations to the $Sq\parallel$ and $Di\parallel$ states are reduced to 1.16 eV and 1.45 eV, respectively, compared with the predictions of 1.9 eV and 2.14 eV derived considering only $\Delta E^{elst}(f)$. Furthermore, the magnitude of $E^{pol}(f)$ is significantly reduced on passing from the \parallel to the \perp excited states explaining why the excitations to the latter final states show only small redshifts of about 0.2 eV compared with that in the bulk crystal. The crystal polarization, in contrast to the dispersive attractions, is a non-additive co-operative phenomenon extending over considerable distances. This observation can rationalize the greater bulk crystal magnitude of $E^{pol}(f)$ compared with those in the encapsulated materials even though the latter polarization has contributions from the nanotube carbon atoms. The greater polarizations in the \parallel final states compared with the \perp ones can be rationalized by noting that in the former the electric fields created by the primary dipole of the metal-halogen pair acts along a chain in the same direction as those created by the dipoles induced on the other ions in the same chain whereas these effects are in opposition in the \perp states.

VI. CONCLUSIONS

For each of the bulk alkali halides, the predicted energy of the longest wavelength transition agrees well with experiment when this excitation is described as a transfer of an anion electron to just one single nearest neighbour cation. This produces the excited state described here as dipolar. The combination of the discussion and numerical results presented in this paper show that three previous criticisms^{21,22} of the charge transfer description of the first excited state cannot be substantiated. The first of these was that the consideration of just the metal ionization potential, halogen electron affinity, and changes in the point charge electrostatic energy could not explain the observed excitation energies. The second criticism was that the first criticism could only be countered by introducing questionable assumptions while the closely related third criticism was that the metal dependent contributions to the excitation energy, that is the term ΔE_M in (6), could not be reliably calculated. We have shown that this term is automatically included without any difficulty in the most accurate theory based on Eq. (5). Furthermore the good agreement with experiment of our numerical predictions derived from (5) using the GULP program provides further evidence in favour of the charge transfer description producing the dipolar excited state while also refuting the criticisms. Three different possible types of excited state in which the halide electron is delocalized over several cation neighbours have been shown to have polarization energies smaller in magnitude than that of the dipolar state thus predicting excitation energies significantly greater than experiment. Arguments have been presented for rejecting a previous suggestion²¹ that the excitation process is purely one-centred. First this approach has been shown to yield values for the excitation energies that are far too small. Second it predicts the wrong number of allowed transitions and, even after introducing spin-orbit coupling, cannot account for the

observed relative intensities of the transitions. An approximate analytic theory based on work^{13,14} dating from the 1930s has been applied to those alkali halides for which GULP computations were inhibited due to the lack of *ab initio* potential data. The resulting predictions were only slightly less accurate than those of the GULP computations thereby showing that these crystals do not constitute any evidence against the dipolar nature of the first excited state.

Encapsulation in a carbon nanotube of an alkali halide crystal produces a nanomaterial consisting of stacks of planes each of which contains four ions. The two lowest energy purely intra-ionic excitations produce dipolar excited states in which the halide electron is transferred to either a cation in the same four ion plane or one in an immediately neighbouring plane. It has been shown that, for encapsulated KI, the point charge electrostatic contribution to each of these excitation energies is approximately 2 eV smaller than in the bulk crystal. This result does not fully transfer to the same reduction of the total excitation energies on encapsulation because the magnitudes of the polarization energies in the excited states of the encapsulated crystals are significantly less than that in the bulk material. However, for the final states in which the electron is transferred to a neighbouring plane, the total excitation energy is reduced by 1.16 eV relative to the bulk if the four ion planes are taken to be square, a possibility consistent with the electron microscopy.² If these planes are taken to have the form slightly distorted to a diamond shape predicted by computations³⁵ using the GULP program, an excitation energy lowering of 1.46 eV is predicted. The polarization energies of the excited states in which the transferred electron remains in the same four ion plane are significantly smaller in magnitude than those of the states in which the electron is transferred to a neighbouring plane. This causes the excitations to the former types of excited state to have energies only about 0.2 eV smaller than that in the bulk crystal.

ACKNOWLEDGMENTS

E.B. is grateful to the Engineering and Physical Research Council (EPSRC) for funding via an EPSRC Career Acceleration Fellowship and New Directions for EPSRC Research Leaders Award (EP/G005060/1). We also thank the Leverhulme Trust for financial support.

¹R. R. Meyer, J. Sloan, R. E. Dunin-Borkowski, A. I. Kirkland, M. C. Novotny, S. R. Bailey, J. L. Hutchinson, and M. L. H. Green, *Science* **289**, 1324 (2000).

²J. Sloan, M. C. Novotny, S. R. Bailey, G. Brown, C. Xu, V. C. Williams, S. Friedrichs, E. Flahaut, R. L. Callender, A. P. E. York, K. S. Coleman, M. L. H. Green, R. E. Dunin-Borkowski, and J. L. Hutchinson, *Chem. Phys. Lett.* **329**, 61 (2000).

³J. Sloan, A. I. Kirkland, J. L. Hutchinson, and M. L. H. Green, *Chem. Commun.* **2002**, 1319.

⁴J. Sloan, S. Friedrichs, R. R. Meyer, A. I. Kirkland, J. L. Hutchinson, and M. L. H. Green, *Inorgan. Chim. Acta* **330**, 1 (2002).

⁵J. Sloan, A. I. Kirkland, J. L. Hutchinson, and M. L. H. Green, *Compt. Rend.* **4**(Pt. 9), 1063 (2003).

⁶E. Philip, J. Sloan, A. I. Kirkland, R. R. Meyer, S. Friedrichs, J. L. Hutchinson, and M. L. H. Green, *Nature Mater.* **2**, 788 (2003).

⁷M. Wilson and P. A. Madden, *J. Am. Chem. Soc.* **123**, 2101 (2001).

⁸M. Wilson, *J. Chem. Phys.* **116**, 3027 (2002).

⁹E. N. Bichoutskaia and N. C. Pyper, *J. Chem. Phys.* **129**, 154701 (2008).

- ¹⁰A. I. Kirkland, W. O. Saxton, and G. Chand, *J. Electron Microsc.* **46**, 11 (1997).
- ¹¹R. R. Meyer, A. I. Kirkland, and W. O. Saxton, *Ultramicroscopy* **92**, 89 (2002).
- ¹²W. Klemm, *Z. Phys.* **82**, 529 (1933).
- ¹³J. H. De Boer, in *Electron Emission and Adsorption Phenomena*, The Cambridge Series in Physical Chemistry, general editor E. K. Rideal (Cambridge University Press, 1935), p. 246 (translated from manuscript by Mrs. H. Tevesacly).
- ¹⁴N. F. Mott, *Trans. Faraday Soc.* **34**, 500 (1938).
- ¹⁵A. W. Overhauser, *Phys. Rev.* **101**, 1702 (1956).
- ¹⁶See supplementary material at <http://dx.doi.org/10.1063/1.4764307> for a brief discussion of, in section A, the inadequacy of the one-centred description of the first excited state in bulk alkali halides, in section B, the details of the calculations of the polarisation responses in the four excited states shown in Figure 2, and, in section C, the details of the inter-species interactions and computational methods.
- ¹⁷G. D. Mahan, *Solid State Ionics* **1**, 29 (1980).
- ¹⁸N. C. Pyper, *Philos. Trans. R. Soc. London, Ser. A* **320**, 108 (1986).
- ¹⁹N. C. Pyper, *Adv. Solid State Chem.* **2**, 223 (1991).
- ²⁰E. N. Bichoutskaia and N. C. Pyper, *J. Phys. Chem. B* **110**, 5936 (2006).
- ²¹D. L. Dexter, *Phys. Rev.* **108**, 707 (1957).
- ²²K. Teegarden and G. Baldini, *Phys. Rev.* **155**, 896 (1967).
- ²³J. D. Gale, *J. Chem. Soc., Faraday Trans.* **93**, 629 (1997).
- ²⁴D. G. Dick and A. W. Overhauser, *Phys. Rev.* **112**, 90 (1958).
- ²⁵F. Seitz, *Modern Theory of Solids* (McGraw-Hill, 1940), Chap. XII, p. 412.
- ²⁶R. L. Lozes, O. Gosinski, and U. I. Wahlgren, *Chem. Phys. Lett.* **63**, 77 (1979).
- ²⁷P. S. Bagus and H. F. Schafer III, *J. Chem. Phys.* **56**, 224 (1972).
- ²⁸*Crystal Structures and Data of Inorganic Compounds*, Landolt-Bornstein New Series III, Vol. 7, Part A, edited by K. H. Hellwege (Springer-Verlag, Berlin, 1973).
- ²⁹N. Jacobi and G. Csanak, *Chem. Phys. Lett.* **30**, 367 (1975).
- ³⁰A. Koide, *J. Phys. B* **9**, 3173 (1976).
- ³¹N. C. Pyper, *Philos. Trans. R. Soc. London, Ser. A* **352**, 89 (1995).
- ³²P. W. Fowler and N. C. Pyper, *Mol. Phys.* **59**, 317 (1986).
- ³³N. C. Pyper and P. Popelier, *J. Phys. Condens. Matter* **7**, 5013 (1995).
- ³⁴N. C. Pyper, *J. Phys. Condens. Matter* **7**, 9127 (1995).
- ³⁵E. N. Bichoutskaia and N. C. Pyper, *J. Chem. Phys.* **128**, 024709 (2008).
- ³⁶N. C. Pyper, A. I. Kirkland, and J. H. Harding, *J. Phys. Condens. Matter* **18**, 683 (2006).
- ³⁷M. P. Housden and N. C. Pyper, *J. Phys. Condens. Matter* **20**, 085222 (2008).
- ³⁸M. Born, cited by J. H. De Boer, in *Electron Emission and Adsorption Phenomena*, The Cambridge Series in Physical Chemistry, general editor E. K. Rideal (Cambridge University Press, 1935), p. 241 (translated from manuscript by Mrs. H. Tevesacly).
- ³⁹C. von Hippel, *Z. Phys.* **101**, 680 (1936).
- ⁴⁰C. Moore, *Atomic Energy Levels as Derived from the Analysis of Optical Spectra*, NBS Circular 467, Vols. 1, 2, and 3 (U.S. Govt. Printing Office, Washington, DC, 1949-1958).
- ⁴¹B. M. Smirnov, *Negative Ions*, Table 1.10, translated by S. Chomet and H. S. W. Massey (McGraw Hill, 1982).
- ⁴²P. W. Fowler and P. A. Madden, *Phys. Rev. B* **29**, 1035 (1984).
- ⁴³P. W. Fowler, P. J. Knowles, and N. C. Pyper, *Mol. Phys.* **56**, 83 (1985).
- ⁴⁴P. W. Fowler and N. C. Pyper, *Proc. R. Soc. London, Ser. A* **398**, 377 (1985).
- ⁴⁵H. J. Werner and W. E. Meyer, *Phys. Rev. A* **13**, 13 (1976).
- ⁴⁶E. A. Reinsch and W. E. Meyer, *Phys. Rev. A* **14**, 915 (1976).
- ⁴⁷T. M. Miller and B. Bederson, *Adv. At. Mol. Phys.* **13**, 1 (1977), citing correspondence from E. A. Reinsch and W. E. Meyer.
- ⁴⁸D. R. Lide, *Handbook of Chemistry and Physics*, 90th ed. (CRC Press, Boca Raton, 2009-2010).
- ⁴⁹J. N. Wilson and R. M. Curtiss, *J. Phys. Chem.* **74**, 187 (1970).
- ⁵⁰E. G. Schneider and H. M. O'Bryan, *Phys. Rev.* **51**, 293 (1937).
- ⁵¹A. J. Dekkar, *Solid State Physics*, Table 15-2 (Macmillan, London, 1962), p. 373.